Waveguide based compact silicon Schottky photodetector with enhanced responsivity in the telecom spectral band

Ilya Goykhman,[1,3] Boris Desiatov,[1†] Jacob Khurgin,[2] Joseph Shappir,[1] and Uriel Levy[1*]

[1]*Department of Applied Physics, The Benin School of Engineering and Computer Science, The Center for Nanoscience and Nanotechnology, The Hebrew University of Jerusalem, Jerusalem, 91904, Israel*
[2]*Department of Electrical and Computer Engineering, Johns Hopkins University, Baltimore, Maryland 21218, USA*
[3]*These authors contributed equally to the work*
[*]*ulevy@cc.huji.ac.il*

Abstract: We experimentally demonstrate an on-chip compact and simple to fabricate silicon Schottky photodetector for telecom wavelengths operating on the basis of internal photoemission process. The device is realized using CMOS compatible approach of local-oxidation of silicon, which enables the realization of the photodetector and low-loss bus photonic waveguide at the same fabrication step. The photodetector demonstrates enhanced internal responsivity of 12.5mA/W for operation wavelength of 1.55μm corresponding to an internal quantum efficiency of 1%, about two orders of magnitude higher than our previously demonstrated results [22]. We attribute this improved detection efficiency to the presence of surface roughness at the boundary between the materials forming the Schottky contact. The combination of enhanced quantum efficiency together with a simple fabrication process provides a promising platform for the realization of all silicon photodetectors and their integration with other nanophotonic and nanoplasmonic structures towards the construction of monolithic silicon opto-electronic circuitry on-chip.

OCIS codes: (040.6040) Detectors; (130.3120) Integrated optics; (240.6680) Surface plasmons.

References

1. Y. Kang, H.-D. Liu, M. Morse, M. J. Paniccia, M. Zadka, S. Litski, G. Sarid, A. Pauchard, Y.-H. Kuo, H.-W. Chen, W. S. Zaoui, J. E. Bowers, A. Beling, D. C. McIntosh, X. Zheng, and J. C. Campbell, "Monolithic germanium/silicon avalanche photodiodes with 340 GHz gain-bandwidth product," Nat. Photonics **3**(1), 59–63 (2009).
2. J. Michel, J. Liu, and L. C. Kimerling, "High-performance Ge-on-Si photodetectors," Nat. Photonics **4**(8), 527–534 (2010).
3. S. Assefa, F. Xia, and Y. A. Vlasov, "Reinventing germanium avalanche photodetector for nanophotonic on-chip optical interconnects," Nature **464**(7285), 80–84 (2010).
4. A. R. Hawkins, W. Wu, P. Abraham, K. Streubel, and J. E. Bowers, "High gain-bandwidth-product silicon heterointerface photodetector," Appl. Phys. Lett. **70**(3), 303–305 (1997).
5. Y. Kang, P. Mages, A. R. Clawson, P. K. L. Yu, M. Bitter, Z. Pan, A. Pauchard, S. Hummel, and Y. H. Lo, "Fused InGaAs-si avalanche photodiodes with low-noise performances," IEEE Photon. Technol. Lett. **14**(11), 1593–1595 (2002).
6. T. K. Liang, H. K. Tsang, I. E. Day, J. Drake, A. P. Knights, and M. Asghari, "Silicon waveguide two-photon absorption detector at 1.5 μm wavelength for autocorrelation measurements," Appl. Phys. Lett. **81**(7), 1323–1325 (2002).
7. T. Tanabe, H. Sumikura, H. Taniyama, A. Shinya, and M. Notomi, "All-silicon sub-Gb/s telecom detector with low dark current and high quantum efficiency on chip," Appl. Phys. Lett. **96**, 101103 (2010).
8. J. D. B. Bradley, P. E. Jessop, and A. P. Knights, "Silicon waveguide-integrated optical power monitor with enhanced sensitivity at 1550 nm," Appl. Phys. Lett. **86**(24), 241103 (2005).
9. J. J. Ackert, M. Fiorentino, D. F. Logan, R. G. Beausoleil, P. E. Jessop, and A. P. Knights, "Silicon-on-insulator microring resonator defect-based photodetector with 3.5-GHz bandwidth," J. Nanophotonics **5**(1), 059507 (2011).

#179284 - $15.00 USD Received 5 Nov 2012; revised 28 Nov 2012; accepted 29 Nov 2012; published 10 Dec 2012

10. K. Preston, Y. H. Lee, M. Zhang, and M. Lipson, "Waveguide-integrated telecom-wavelength photodiode in deposited silicon," Opt. Lett. **36**(1), 52–54 (2011).
11. H. Chen, X. Luo, and A. W. Poon, "Cavity-enhanced photocurrent generation by 1.55 μm wavelengths linear absorption in a p-i-n diode embedded silicon microring resonator," Appl. Phys. Lett. **95**(17), 171111 (2009).
12. M. Casalino, G. Coppola, M. Iodice, I. Rendina, and L. Sirleto, "Critically coupled silicon Fabry-Perot photodetectors based on the internal photoemission effect at 1550 nm," Opt. Express **20**(11), 12599 (2012).
13. D. W. Peters, "An infrared detector utilizing internal photoemission," Proc. IEEE **55**(5), 704–705 (1967).
14. S. M. Sze and K. Ng, Kwok, "Physics of Semiconductor Devices," Wiley, New York (2006).
15. S. Zhu, M. B. Yu, G. Q. Lo, and D. L. Kwong, "Near-infrared waveguide-based nickel silicide Schottky-barrier photodetector for optical communications," Appl. Phys. Lett. **92**(8), 081103 (2008).
16. M. Casalino, L. Sirleto, M. Iodice, N. Saffioti, M. Gioffrè, I. Rendina, and G. Coppola, "Cu/p-Si schottky barrier-based near infrared photodetector integrated with a silicon-on-insulator waveguide," Appl. Phys. Lett. **96**(24), 241112 (2010).
17. J. E. Sipe and J. Becher, "Surface-plasmon-assisted photoemission," J. Opt. Soc. Am. **71**(10), 1286–1288 (1981).
18. J. G. Endriz, "Surface waves and grating-tuned photocathodes," Appl. Phys. Lett. **25**(5), 261–262 (1974).
19. Y. Wang, X. Su, Y. Zhu, Q. Wang, D. Zhu, J. Zhao, S. Chen, W. Huang, and S. Wu, "Photocurrent in Ag-Si photodiodes modulated by plasmonic nanopatterns," Appl. Phys. Lett. **95**(24), 241106 (2009).
20. A. Akbari and P. Berini, "Schottky contact surface-plasmon detector integrated with an asymmetric metal stripe waveguide," Appl. Phys. Lett. **95**(2), 021104 (2009).
21. A. Akbari, R. N. Tait, and P. Berini, "Surface plasmon waveguide schottky detector," Opt. Express **18**(8), 8505–8514 (2010).
22. I. Goykhman, B. Desiatov, J. Khurgin, J. Shappir, and U. Levy, "Locally oxidized silicon Surface-Plasmon schottky detector for telecom regime," Nano Lett. **11**(6), 2219–2224 (2011).
23. T. Aihara, K. Nakagawa, M. Fukuhara, Y. L. Yu, K. Yamaguchi, and M. Fukuda, "Optical frequency signal detection through surface plasmon polaritons," Appl. Phys. Lett. **99**(4), 043111 (2011).
24. M. Fukuda, T. Aihara, K. Yamaguchi, Y. Y. Ling, K. Miyaji, and M. Tohyama, "Light detection enhanced by surface plasmon resonance in metal film," Appl. Phys. Lett. **96**(15), 153107 (2010).
25. M. W. Knight, H. Sobhani, P. Nordlander, and N. J. Halas, "Photodetection with active optical antennas," Science **332**(6030), 702–704 (2011).
26. S. Zhu, H. S. Chu, G. Q. Lo, P. Bai, and D. L. Kwong, "Waveguide-integrated near-infrared detector with self-assembled metal silicide nanoparticles embedded in a silicon p-n junction," Appl. Phys. Lett. **100**(6), 061109 (2012).
27. B. Desiatov, I. Goykhman, and U. Levy, "Demonstration of submicron square-like silicon waveguide using optimized LOCOS process," Opt. Express **18**, 18592–18597 (2010).
28. P. B. Johnson and R. W. Christy, "Optical constants of the noble metals," Phys. Rev. B **6**(12), 4370–4379 (1972).
29. H. Norde, "A modified forward I-V plot for schottky diodes with high series resistance," J. Appl. Phys. **50**(7), 5052–5053 (1979).
30. S. K. Cheung and N. W. Cheung, "Extraction of schottky diode parameters from forward current-voltage characteristics," Appl. Phys. Lett. **49**(2), 85–87 (1986).
31. K. Sato and Y. Yasumura, "Study of forward I-V plot for schottky diodes with high series resistance," J. Appl. Phys. **58**(9), 3655–3657 (1985).
32. H. C. Card, "Aluminum-Silicon schottky barriers and ohmic contacts in integrated circuits," IEEE Trans. Electron. Dev. **23**(6), 538–544 (1976).
33. Z. Horváth, M. Ádám, I. Szabó, M. Serényi, and V. Van Tuyen, "Modification of Al/Si interface and schottky barrier height with chemical treatment," Appl. Surf. Sci. **190**(1-4), 441–444 (2002).
34. V. M. Shalaev, C. Douketis, J. T. Stuckless, and M. Moskovits, "Light-induced kinetic effects in solids," Phys. Rev. B **53**(17), 11388–11402 (1996).
35. I. Schnitzer, E. Yablonovitch, C. Caneau, T. J. Gmitter, and A. Scherer, "30% external quantum efficiency from surface textured, thin-film light-emitting diodes," Appl. Phys. Lett. **63**(16), 2174–2176 (1993).
36. T. Fujii, Y. Gao, R. Sharma, E. L. Hu, S. P. DenBaars, and S. Nakamura, "Increase in the extraction efficiency of GaN-based light-emitting diodes via surface roughening," Appl. Phys. Lett. **84**(6), 855–857 (2004).
37. R. H. Horng, S. H. Huang, C. C. Yang, and D. S. Wuu, "Efficiency Improvement of GaN-Based LEDs with ITO Texturing Window Layers Using Natural Lithography," IEEE J. Sel. Top. Quantum Electron. **12**(6), 1196–1201 (2006).

1. Introduction

Realization of silicon-based photodetectors for telecom wavelengths using mature and well established CMOS technology is an essential step toward on-chip monolithic integration of optical communication systems with modern electronic circuitry. While silicon photodetectors are widely used in the visible spectral range, they are not suitable for detecting near-infrared radiation at the telecom wavelength region (1.3-1.6 um). This is simply because the energy of an infrared photon is not sufficient to overcome the potential barrier of silicon

#179284 - $15.00 USD Received 5 Nov 2012; revised 28 Nov 2012; accepted 29 Nov 2012; published 10 Dec 2012

bandgap (1.1eV) and thus there is no photogeneration of free carriers via intraband transitions. Over the years, the silicon photonics industry developed solutions for circumventing this deficiency, e.g. by applying an active layer of germanium into the silicon structure [1–3] and by employing wafer bonding technology for integration of compound semiconductors [4, 5] with silicon platform. While these approaches provide a path towards detection of light at the telecom spectral range, there is still a clear advantage in developing monolithic CMOS compatible all-silicon photodetectors, without the requirement to rely on other material systems. Motivated by this need, a number of silicon based photo detectors operating in the near infrared were proposed and demonstrated. Several photodetection mechanisms have been considered, including two-photon absorption [6, 7], insertion of midbandgap defect states into the silicon lattice [8,9], using a deposited polysilicon active layer [10] and enhancing these relatively weak processes by using the concept of cavity enhanced photocurrent generation [7,9–12].

Another promising approach to detect infrared sub-bandgap optical radiation in silicon is to employ the internal photoemission (IPE) process using a Schottky type photodetector [13–16]. In its simplest form, this device consists of a metal film on a lightly doped semiconductor (e.g. silicon) forming a Schottky contact at the metal-semiconductor interface with potential barrier Φ_B and rectifying electrical characteristics. Usually, the obtained Schottky barrier (SB) is lower than the energy bandgap of silicon [13], thus allowing internal photoemission of conduction electrons from the metal to the semiconductor upon the absorption of infrared photons with energy $h\nu$ exceeding the potential barrier at the interface. The main advantages of such device reside in its simple fabrication, large bandwidth, and intrinsically high frequency response due to the fast thermalization time (ca. few picoseconds) of excited electrons in the metal. On the other hand, the drawback of Schottky type photodetector originates from low efficiency of the IPE process, since the volume in which electro-magnetic energy interacts with electrons in the metal is very small, only a small fraction of the incident photons actually causes photoemission. Moreover, being excited in the metal with huge Fermi wavevector and tending to be emitted into semiconductor, the “hot“ electrons typically acquire low transmission probability because of considerable momentum mismatch and poor overlap of the electron wavefunctions between the metal and the semiconductor.

One way to enhance the IPE process efficiency is to concentrate optical electromagnetic energy at the boundary between the metal and the semiconductor, were the Schottky contact is formed, thereby increasing light interaction with electrons in the vicinity of the interface where photoemission process takes place [17, 18]. Following this concept, several infrared Schottky photodetectors in silicon were recently presented taking advantage of the high field confinement of surface plasmons at the metal-semiconductor interface [19–26]. Two major configurations were explored in these demonstrations. One takes advantage of the enhanced absorption in the vicinity of a Schottky contacts via the excitation of localized plasmons, e.g. by using nanoantennas or metallic nanoparticles [24–26], while the other is based on guiding of electro-magnetic energy along the Schottky interface utilizing the well confined surface plasmon polariton (SPP) waves [19–23]. The guided mode approach typically offers longer interaction length between the propagating SPP and the photodetector, thus allowing larger portion of the optical energy to be absorbed nearby the Schottky barrier. This combination of efficient optical absorption and light confinement enhances the detection capabilities of the system and potentially pave the way to device miniaturization and dense on-chip integration.

In this work we demonstrate a compact, simple and efficient Schottky photodetector for telecom wavelengths. The device is integrated with a nanoscale silicon bus waveguide and may serve as a building block of an on chip optical receiver. Interestingly, the demonstrated photodetector shows internal quantum efficiency of about two orders of magnitude higher than our previous demonstration [22]. Potential explanation for this enhancement will be discussed later on in the text.

#179284 - $15.00 USD Received 5 Nov 2012; revised 28 Nov 2012; accepted 29 Nov 2012; published 10 Dec 2012

2. Device fabrication

Our device is realized using the standard microelectronic technique of local–oxidation of silicon (LOCOS), in which the photonic circuitry is defined by the oxide spacers rather than the reactive ion etching (RIE). Implementation of local-oxidation process provides CMOS compatibility and enables realization of low loss photonic waveguides with precise control over the shape, dimensions and cross sectional profile of the optical structure [27]. We used silicon on insulator (SOI) substrate with 340nm-thick p-type silicon device layer ($0.2\ \Omega \cdot cm$) on top of 2μm-thick buried oxide. First, 120nm thick layer of silicon nitride (SiN) was deposited by low-pressure chemical vapor deposition (LPCVD) at $800^{\circ}C$. Next, the oxidation mask defining the optical and electrical structures of the opto-electronic link was patterned in electron beam resist (ZEP 520) using standard electron-beam lithography (EBL, Raith eLine 150). The mask was transferred into the SiN layer by reactive ion etching (RIE, Oxford Plasmalab 100) with a CHF_3/O_2 gas mixture. The defined pattern was transferred to the silicon by LOCOS process at $1000^{\circ}C$, namely the local-oxidation takes place only in the areas where silicon is exposed to the oxygen, while at the same time the SiN protective layer serves as a mask preventing O_2 diffusion into the silicon and further oxide growth. After the oxidation, in order to uncover the silicon interface for the purpose of forming the Schottky contact, the sacrificial SiN mask layer as well as the thermally grown LOCOS oxide were removed by wet etching in hot phosphoric acid and hydrofluoric acid respectively. To integrate the Schottky device with the photonic waveguide we first realized an ohmic contact to silicon by evaporating an aluminum pad and alloying the structure at $420^{\circ}C$ in H_2/N_2 ambient condition. Finally, the Schottky contact was laid down over the photonic structure by the lift-off of 100nm-thick aluminum strip intersecting the silicon waveguide. A scanning electron microscope (SEM) micrograph of the fabricated device is presented in Fig. 1. The photodetector length is only 1 μm, and the obtained dimensions of photonic bus waveguide are 305nm-width and 340nm-height, supporting a single TM (out of plane) polarized optical mode. As evident from Fig. 1, that metal line fully covers the waveguide and allows the formation of a continuous and uniform Schottky contact all over the exposed silicon surface. The realization of Schottky contact over the entire waveguide cross section expands the photodetection area where the absorbed optical signal can potentially contribute to the photocurrent compared with our previously demonstrated devices, in which the Schottky contact was formed only on the top layer of the waveguide [22].

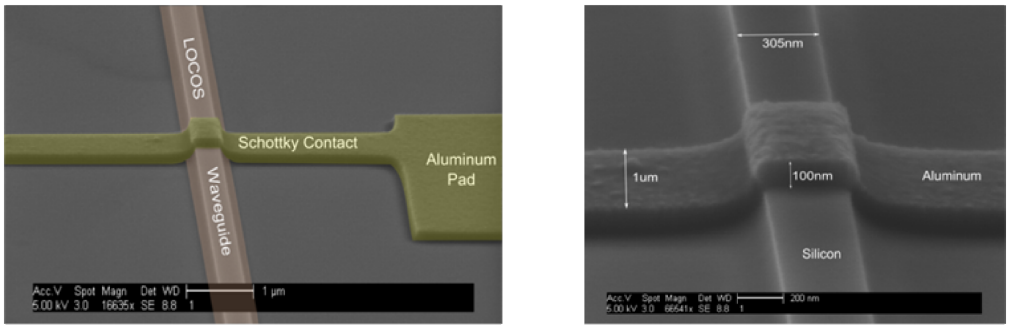

(a) (b)

Fig. 1. a) SEM micrograph of the locally-oxidized silicon bus waveguide integrated with the Schottky photodetector. b) Zoom in on the Schottky contact. The scale bars shown are relevant only for a lateral dimension because of the slanted view of the micrographs. The scale bar for the vertical direction should be corrected by taking into account a tilt angle of 20 degrees.

#179284 - $15.00 USD Received 5 Nov 2012; revised 28 Nov 2012; accepted 29 Nov 2012; published 10 Dec 2012

3. Numerical simulations

Two of the most important characteristics of a photodetector are its quantum efficiency and responsivity. In order to estimate these parameters, one needs to know the amount of optical power absorbed in the device. In the following section we aim at estimating the absorption and transmission properties of the fabricated Schottky structure. Taking into account the actual dimensions of photodetector as measured from the SEM image and assuming the operation wavelength of 1.55μm with out-of-plane (TM) polarization, we simulated the optical mode profile of the bus waveguide and the plasmonic structure of the Schottky contact using the finite-element mode solver (COMSOL). As shown in Figs. 2a and 2b, the effective refractive indexes of the photonic and the plasmonic modes were found to be 2.39 and 2.64 + 0.047i respectively. From these results one can estimate the portion of light which is absorbed by the metal. Considering the negligible Fresnel reflection due to impedance mismatch (about 0.25% per facet), the overlap between the two modes (found by overlap integral to be 62%) and the SPP propagation length of 2.6μm we estimated the optical power transmitted though the device to be ~25% with respect to the optical power propagating in the photonic bus waveguide. The remaining 75% is split between radiation of light due to mode mismatch (over 50%) and absorption in the Schottky structure as a result of the ohmic loss in the metal (~22%).

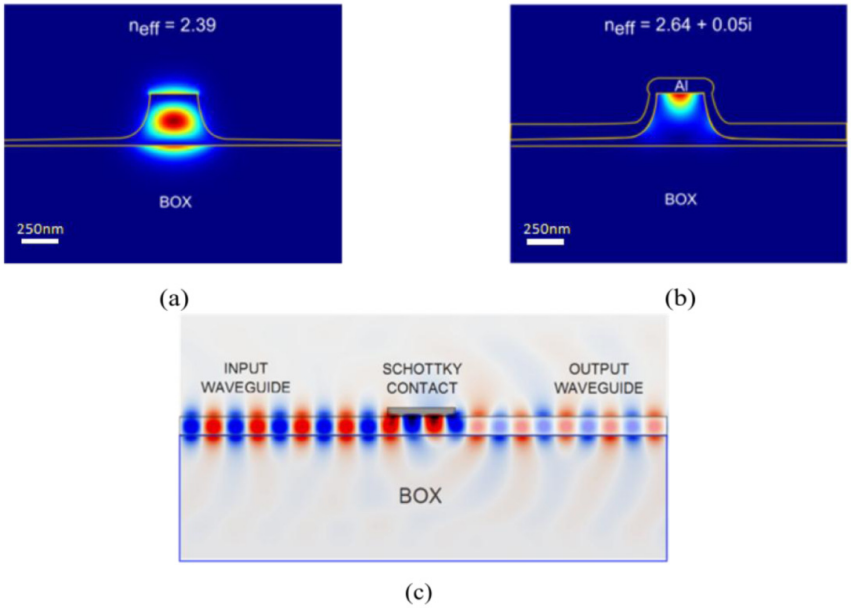

Fig. 2. a) Intensity profile of the optical mode resides in the photonic bus waveguide. b) Intensity profile of the plasmonic mode resides in the Schottky contact. c) Vertical cross section of the out of plane electric field distribution at the center of the device along the propagation direction, as calculated by 3D FDTD simulation

To confirm these calculations we carried out a three dimensional (3D) final-difference time-domain (FDTD) simulation of the device. The aluminum permittivity was assumed to follow the Drude model, including damping [28]. Figure 2c shows a snapshot of the electric field distribution (out of plane component) along the light propagation direction at the center width of the device. Following the calculation of the power flux in the bus waveguide after the Schottky contact and its normalization with respect to the same waveguide with no Schottky contact we found the total power transmission through the device to be ~30%, very similar to the value expected from the previous estimate which was based on mode mismatch and attenuation.

#179284 - $15.00 USD Received 5 Nov 2012; revised 28 Nov 2012; accepted 29 Nov 2012; published 10 Dec 2012

4. Near-field characterization

To test our numerical expectation we performed near field optical characterization of the photodetection area with near field scanning optical microscope (NSOM, Nanonics MultiView 4000). A representative scan is shown in Fig. 3. Using a metal coated NSOM tip with an aperture diameter of 250nm, we collected the near-field intensity distribution in the vicinity of photodetector. By calculating the ratio between the incoming and outgoing average optical power as it was measured in the bus waveguide slightly before and after the photodetector, we appraised the optical loss to be in the order of 3.5 ± 0.6dB. This value, obtained by an average of dozen independent measurements over 4 different devices, is in reasonable agreement with our simulation prediction of ca. 30% of optical transmission through the device.

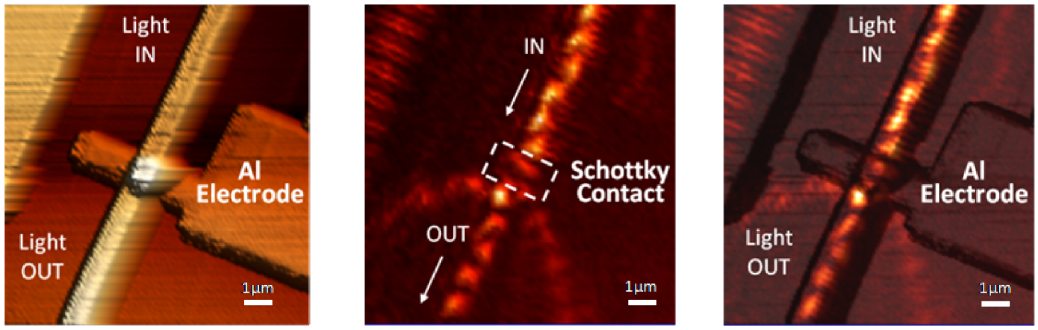

Fig. 3. Near-field characterization of Schottky photodetector. a) Topography image; b) NSOM image; c) 3D representation of the superimposed topography and NSOM images.

5. Electrical and optical characterizations

The electrical properties of the Schottky contact were derived from the temperature dependent current-voltage (I-V) measurements. As shown in Fig. 4, the device demonstrates rectifying characteristics (e.g. diode) with the forward bias region limited by serial resistance of the contact (~24KΩ) and leakage current in the order of 30nA for reverse bias of 0.1V. As expected from Schottky diode thermal dependence [14], the reverse current across the photodetector is increased with temperature due to enhanced thermionic emission of metal electrons into the silicon. In this operation mode, the variations of reverse leakage current are reflected to the forward bias region, as it is evident from Fig. 4. Using experimental data, the electrical parameters of the Schottky contact were extracted by exploiting the modified Norde method [29–31]. With this approach, the potential barrier height at the interface, the ideality factor and the serial resistance were found to be $\Phi_B = 0.42\,eV$, n = 1.8 and $R_S = 24\,K\Omega$ respectively. The obtained Schottky barrier of 0.42eV is very similar to the values presented in literature for p-type silicon - aluminum contact [32,33].

#179284 - $15.00 USD Received 5 Nov 2012; revised 28 Nov 2012; accepted 29 Nov 2012; published 10 Dec 2012

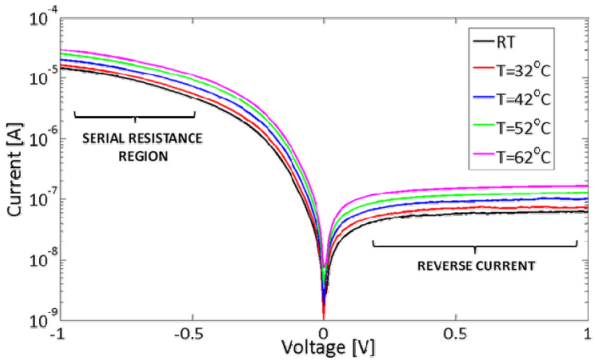

Fig. 4. Temperature dependent electrical characterization of the device

The detection capability of the device was tested by measuring the I-V characteristics of the integrated Schottky detector at the presence of optical signal. A 1.55μm wavelength TM polarized light was butt coupled to the photonic bus waveguide using a polarization maintained lensed fiber with a mode size of ~2.5μm. At the output facet the optical signal was collected with a similar fiber and detected by an external InGaAs photodetector. Our sample consists of a symmetric Y-branch to split optical signal between the Schottky photodetector and a reference waveguide, which in turn was continuously monitored in order to preserve constant coupling conditions during the experiment. To obtain the responsivity, we measured I-V curves of the Schottky photodetector for different optical power coupled to the Schottky region (Fig. 5a), and plotted the current values at small reverse bias of 0.1V as a function of optical power inside the SPP waveguide (Fig. 5b).

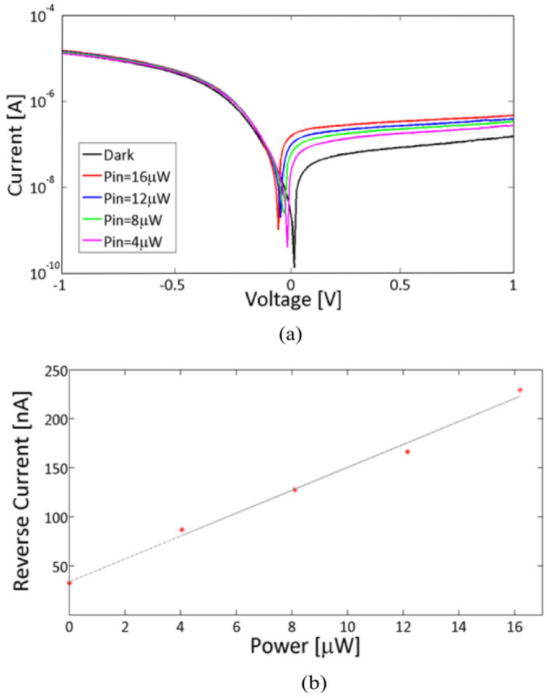

Fig. 5. Opto-electronic characterization of the integrated Schottky photodetector. a) I-V measurements as a function of the incident optical power at operation wavelength of 1.55μm. b) The responsivity plot of the device at operation wavelength of 1.55μm. The reverse current is taken for a small reverse bias of 0.1V.

#179284 - $15.00 USD Received 5 Nov 2012; revised 28 Nov 2012; accepted 29 Nov 2012; published 10 Dec 2012

Based on Fig. 5a, the device operates in photoconductive mode, where a higher optical signal affects primarily the reverse bias region, since the photogeneration process acts as an external current source added on top of the leakage (dark) current of the diode. As expected in this case, the reverse current across the contact grows linearly with respect to the increase in optical power (Fig. 5b) and the slope of the curve corresponds to the internal responsivity of the device according to $I_R = I_{dark} + R \cdot P_{in}$, where I_{dark} is the leakage current of the diode, R is the photodetector responsivity and Pin is the optical power coupled to the SPP waveguide. Taking into account ~17.5dB coupling loss between the external tapered fiber and silicon waveguide (as it was measured by monitoring the output signal in the reference waveguide), a typical propagation loss of our LOCOS waveguide measured to be lower than 0.1dB/mm, a 3dB power splitting in the Y-branch and ca. 60% coupling efficiency from the bus silicon waveguide to the SPP waveguide, we estimated the maximal optical power within the Schottky detector to be in the order of 16μW for an incident laser power of 4mW. Consequently, according to Fig. 5b the internal responsivity of our photodetector at the wavelength of 1.55 μm is 12.5mA/W which corresponds to an internal quantum efficiency of about 1%. Taking into account that only ~1/3 of the optical power which is coupled to the Schottky structure is actually absorbed in the device, we believe that the internal quantum efficiency may be even higher, in the order of 3%. It should be noted, that due to significant coupling loss between the lensed fiber and photonic bus waveguide the external quantum efficiency of the device is about two orders of magnitude lower than the internal one, however it could be significantly improved by employing coupling optimization based-on the inverse taper or grating coupler approaches. By doing so, and by using a longer device in which most of the incident optical power is absorbed in the Schottky contact, the responsivity at this wavelength can reach 30-40 mA/W.

Finally, the obtained internal quantum efficiency of 1-3% demonstrates about two orders of magnitude improvement compared to our previously reported results [22], where the integrated Schottky photodetector was realized on top of the atomically flat silicon surface of the bus waveguide. This significant increase cannot be explained only in terms of potential barrier variation or minor area differences between the devices. We attribute the enhancement of internal quantum efficiency to the fact, that in current work the Schottky contact is formed around the silicon waveguide including the waveguide sidewalls which are rough at the atomic scale. This surface roughness originates from SiN mask imperfections on the scale of 1-5nm. While consecutive oxidation is expected to smoothen the silicon waveguide surface, it is still rough on the scale of few atoms. The appearance of surface roughness at the metal-silicon contact may improve the efficiency of the internal photoemission process due to the presence of localized, high density electric fields at the sharp edges of surface imperfections, thereby locally intensifying the Schottky effect of potential barrier lowering. The second, and perhaps the most important beneficial impact of roughness is that it relaxes the momentum conservation [34] rules at the interface and thus allows the photoexcited electrons that otherwise would have been totally reflected back into the metal, to enter the semiconductor. The surface roughness acts upon the electrons attempting to exit across the Schottky barrier exactly as it acts upon the photons trying to exit the semiconductor in light emitting diodes [35–37] and thus plays a similar beneficial role in enhancing the efficiency.

6. Conclusions

In summary, we experimentally demonstrated an on-chip compact, simple and efficient Schottky photodetector for telecom wavelengths integrated with the nanoscale silicon bus waveguide. The fabricated device exhibits the enhanced detection capabilities and shows internal responsivity of 12.5mA/W which is correspondent to the internal quantum efficiency of 1%. With our present device, the efficiency of IPE process is greatly improved (ca. two orders of magnitude) compared to our previously demonstrated results. We attribute this enhancement to the presence of surface roughness at the metal-silicon interface forming the

#179284 - $15.00 USD Received 5 Nov 2012; revised 28 Nov 2012; accepted 29 Nov 2012; published 10 Dec 2012

Schottky contact. It is our hope that the demonstrated device would serve as a step forward in the effort of merging silicon nanophotonic and silicon plasmonic platforms, with the major goal of using silicon nanostructures for the detection of optical signals at the telecom regime.

Acknowledgments

We acknowledge a technical support of Mrs. Noa Mazursky. The research was partially supported by US-Israel Binational science foundation and by Focal Technology Area on Nanophotonics for Detection. I.G and B.D acknowledge financial support from the Eshkol Fellowship. The devices were fabricated at the Center for Nanoscience and Nanotechnology, The Hebrew University of Jerusalem.

#179284 - $15.00 USD Received 5 Nov 2012; revised 28 Nov 2012; accepted 29 Nov 2012; published 10 Dec 2012